I&EC research
Industrial & Engineering Chemistry Research

Article

pubs.acs.org/IECR

Solvent Free Generation of Open and Skinless Foam in Poly(L-lactic acid)/Poly(D,L-lactic acid) Blends Using Carbon Dioxide

Xia Liao*[,†,‡] and Arghavan V. Nawaby[‡,§]

[†]College of Polymer Science and Engineering, Sichuan University, Chengdu, 610065, China

[‡]Institute for Chemical Process and Environmental Technology, National Research Council of Canada, Ottawa, Ontario K1A 0R6, Canada

ABSTRACT: Foams generated via carbon dioxide (CO_2) processing typically exhibit a solid skin layer on the exterior surface and a closed-pore structure with limited interconnectivity in the core section thus limiting its application for biomedical intent. By controlling the properties of poly(L-lactic acid)/poly(D,L-lactic acid) (PLLA/PDLLA) blends and using CO_2 with specific processing parameters, skinless foams with interconnected porous structure were prepared in this work using only CO_2 as a physical foaming agent, which overcome the necessity to use organic solvents and solid porogens. The crystallization behaviors and sorption kinetics of PLLA and its blends were studied. Addition of PDLLA reduces the crystallinity of PLLA/PDLLA blends while treated with CO_2 as compared to neat PLLA. The solubility and diffusion coefficients of CO_2 in PLLA and its blends were found to be similar. Furthermore, the effect of PLLA/PDLLA blend ratio and CO_2 treatment conditions on the foam morphologies was investigated. Through fine parameter control, well interconnected pore structures with a porous surface were generated. Results indicated that by controlling the physical properties of samples combined with optimizing CO_2 foaming process, it is indeed possible to create biodegradable interconnected porous structures for potential biomedical applications.

1. INTRODUCTION

Porous, biodegradable polymer matrices have been extensively utilized as a three-dimensional extracellular matrix analogue for regeneration of various tissues.[1] However, most of the existing fabrication techniques such as solvent casting/salt leaching, emulsion freeze-drying, phase separation, fiber forming, and three-dimensional (3D) printing for generation porous biodegradable scaffolds[2,3] require the use of organic solvents that may not be able to completely be removed. The residual organic solvents in the matrices may induce biocompatibility problems. From a biomedical standpoint, it is clearly desirable to use nontoxic solvents for generation of biodegradable porous materials.

Using the CO_2 gas foaming method to create interconnected porous structures would be an obvious choice to overcome the limitation. Treatment of polymers with CO_2 gas has been an area of investigation for decades, and foam morphologies with various industrial applications has been successfully processed.[4,5] In CO_2 gas foaming, pores are created by either reducing pressure (pressure quench method) or increasing temperature (temperature soak method) that induces thermodynamic instability and thus bubble nucleation. The residual CO_2 in the morphology after foaming process is eventually replaced by air due to a concentration gradient with the surrounding environment.[6] Manipulations of the processing parameters such as pressure, temperature, and pressure drop rate can result in formation of distinctive morphologies.[4]

In addition to its use as an environmentally friendly and economic solvent, CO_2 may also be utilized to purify a matrix via extraction.[7] In this respect, fabrication of porous biopolymers under organic solvent-free conditions combined with possible extraction of impurities from the polymer matrix shows great potential for bioengineering applications. Morphologies of a number of biopolymers such as poly(D,L-lactic-co-glycolic acid) (PLGA),[8] poly(ester amide) (PEA),[9] poly(L-lactic acid) (PLLA),[8,10,11] poly(lactic acid) (PLA),[12] poly(D,L-lactic acid) (PDLLA),[8] polycaprolactone (PCL),[13,14] PCL/ nanocomposites,[15] and copolymer of ω-pentadecalactone (PDL) and ε-caprolactone (CL) (poly(PDL-CL)),[16] and so forth have been investigated using CO_2 as a "green" foaming agent. However, for biomedical applications, the disadvantage of the CO_2 foaming process is that the foams typically exhibit a solid skin layer on the exterior surface and closed pores in the core section. In biopolymer−CO_2 systems aimed at bioengineering applications lack of pore interconnectivity and an unfoamed skin layer can hamper cell seeding, tissue growth, and vascularization. To improve pore interconnectivity, approaches such as CO_2 gas foaming with particulate leaching,[17−20] particle seeding,[21] and CO_2 solid-state foaming with ultrasound to break the pore walls[22] were utilized. Ethanol used as a cosolvent with supercritical CO_2 was also applied in the preparation of the skinless poly(methyl methacrylate) (PMMA) foams.[23]

Among the biopolymer−CO_2 systems investigated, PLA remains an attractive choice because it is producible from renewable resources, nontoxic, and biodegradation attribute in human body. PLA is one of a few chiral polymers, and the stereochemical structure can easily be modified by polymerizing a controlled mixture of the L- and D-isomers to yield high molecular weight amorphous or crystalline polymers.[24] Poly (L-lactic acid) (PLLA) comprises isotactic sequences and therefore

Received: January 11, 2012
Revised: April 13, 2012
Accepted: April 18, 2012
Published: April 18, 2012

dx.doi.org/10.1021/ie3000997 | *Ind. Eng. Chem. Res.* 2012, 51, 6722−6730

are crystallizable, whereas poly (D,L-lactic acid) (PDLLA) is composed of a racemic mixture of L- and D-lactides and therefore is amorphous.[25] Crystallinity in PLLA results in a higher modulus and strength but also brittle nature and a lack in toughness. In contrast, due to the amorphous nature, PDLLA has lower modulus but higher degradability than PLLA.[26] In order to improve the flexibility, toughness, and crystallinity in PLLA, copolymerizing or blending with other polymers has been attempted.[27] Polymer blending in some cases remains a much more cost-effective approach than copolymerization. Thus, blending is a more frequently used and common method to optimize material properties such as processability, rigidity, impact and tensile strength, barrier properties, crystallinity, and degradation rate. Baratian et al.[28] have reported that the presence of random D-lactide decreased the degree of crystallinity and spherulite growth rates in PLLA. Therefore, biomaterials with controlled and improved performance can be obtained by blending PLLA and PDLLA, in which faster degradability of PDLLA allows the ingrowth of cells and addition of PLLA ensures mechanical stability needed in the matrix.[29]

While developing foam structures, the physical property changes induced by CO_2 in the treatment process plays an important role in the resultant morphologies. Gas induced crystallization in PLLA−CO_2 system resulted in unique morphologies with a porous core and a porous skin layer with interconnected pores.[10,11] By controlling the melt strength and crystallization behavior of PLA, PLA foams with interconnected structures were obtained at foaming temperatures between 90 and 105 °C.[30] Open pore morphologies of PLA also could be generated by extrusion foaming method.[31,32] Comparatively, amorphous PDLLA processed with CO_2 exhibited foam morphologies that consisted of closed pores and a nonporous skin layer.[8] It has been reported blending atactic polystyrene (PS) with syndiotactic polystyrene (sPS)[33] and isotactic poly(methyl methacrylate) (*it*-PMMA) with syndiotactic poly(methyl methacrylate) (*st*-PMMA)[34] resulted in superior microporous structures using CO_2 foaming method. Therefore, it is expected that performance improvements can be obtained when particular and targeted polymer blends such as PLLA/PDLLA are treated with CO_2 gas. Although by combining particulate leaching technique, ultrasound, and ethanol with the gas foaming process, the porosity and interpore connectivity of polymer foams can be significantly improved, complete elimination of closed pores remains challenging. To the best of our knowledge, preparation of the skinless foam with interconnected porous structure using only CO_2 as agent in the foaming process has not been reported. In this work, morphologies with open and interconnected core and no skin on the outer layer is produced by simply controlling the physical properties of PLLA/PDLLA blends and CO_2 processing parameters without using any other additives or solvents.

2. EXPERIMENTAL SECTION

2.1. Materials. PLLA pellets (lot no. API-092804−1, M_w = 58 700, M_w/M_n = 1.8, density = 1.24 g/cm^3, T_g = 50 °C, T_c = 88 °C, and T_m = 168 °C), and PDLLA pellets (lot no. API-083104−1, M_w = 36 000, M_w/M_n = 2.4, density = 1.25 g/cm^3, and T_g = 43 °C) were supplied by Birmingham Polymer Inc. Polystyrene (PS) (C-35, M_w = 285 000, density = 1.05 g/cm^3, T_g = 104 °C) was obtained from Scott. Bone-dry 99% pure CO_2 was used.

Blends of PLLA/PDLLA in the ratios of 90/10, 70/30, 50/50, and 30/70 wt % were prepared by melt processing using a Minlab microcompounder (Thermo HAAKE Rheomex CTW5) at 190 °C while recirculated for 2 min in the mixer.

PLLA, PLLA/PDLLA blends, as well as PS samples in sheets about 280 μm thick were prepared by compression molding at 190 °C under 20 MPa for 5 min using a hydraulic heated press machine (Carver Inc.) and subsequently quenching the samples in ice−water.

2.2. Thermal Analysis. Thermal analyses were carried out using thermogravimetry (TGA Q500) and differential scanning calorimetry (DSC 2920) on a TA Instruments. All measurements were performed under nitrogen. In this study, the thermal degradation behaviors of the samples were recorded with heating samples from room temperature to 400 °C at a rate of 10 °C/min. DSC measurements were carried out by heating samples from room temperature to 190 °C at a rate of 5 °C/min and held for 2 min to erase the thermal history. Subsequently, the samples were quenched to 25 °C by liquid nitrogen and then reheated to 190 °C at a heating rate of 5 °C/min. The second heating run of the DSC curves were used to analyze the thermal property of the samples.

2.3. CO_2 Induced Crystallization. A Bruker GADDS diffraction system using Co Kα with a 2D HISTAR detector was used to investigate the physical characteristics of the compression molded samples before and after treatment with CO_2 gas. CO_2 conditioned samples were prepared by saturating the films at 0 °C and 2.8 MPa for 24 h. A period of 24 h was used, since complete equilibrium in the polymer−gas system was reached as revealed by the sorption experiments for the tested samples of comparable thickness. Following the saturation step, the pressure in the saturation vessel was rapidly released, and samples were aged for at least 5 days prior to obtaining the X-ray diffraction patterns. The crystalline volume fraction in the semicrystalline samples were then determined from the diffracted intensity patterns by comparing the relative area under the crystalline peaks to that of the amorphous area.

2.4. Gas Solubility Measurements. CO_2 sorption kinetic studies were carried out using a CAHN D110 microbalance and a previously established method.[35] Polymer sample (0.3 g) was loaded in the balance, and the system was pressurized to the desired value at 0 °C. The changes in the polymer mass as a result of gas uptake were recorded as a function of time and a period of 24 h was required for the system to reach equilibrium. Blank runs under the same experimental conditions provided the balance zero-shift as a function of pressure, and equilibrium mass readings were corrected for the zero-shift. Buoyancy corrections were also applied to the solubility data, since a small volume difference between the sample and reference side in the balance develops due to gas dissolution in the polymer resulting in dilation of the matrix.[35] The CO_2 densities used for buoyancy corrections were obtained from tables for IUPAC recommended equations of state.[36] Diffusion coefficients of the gas in the polymer were subsequently derived from the corrected sorption kinetic data using a nonlinear regression program.[37]

2.5. Foaming and Foam Characterization. Foamed specimens were prepared using the temperature soak method on a batch foaming system. The blend samples were put into an autoclave and saturated with CO_2 at 0 °C and 2.8 MPa for 24 h. Subsequently, the gas pressure was released (in 5 s), and the samples were transferred rapidly to a preheated water bath in the range 30−100 °C and foamed for 30 s. After the foaming

dx.doi.org/10.1021/ie3000997 | Ind. Eng. Chem. Res. 2012, 51, 6722−6730

process, samples were quenched in ice water to freeze the foam morphology. The foamed samples were fractured using liquid nitrogen and sputter-coated with Au/Pd. The foam morphologies on the cross section and surface of the samples were imaged using JEOL JSM 840A field emission scanning electron microscopy (SEM).

The porosity (P) of the scaffolds was determined by measuring the dimensions and the mass of the scaffold using eq 1:

$$P = \left[1 - \frac{d_p}{d}\right] \times 100 \quad (1)$$

where d_p is the scaffold density and d is the density of a nonporous sample before conditioning with CO_2, which were determined by measuring the mass in air and in water using an electronic balance with a resolution of ±10 μg.

3. RESULTS AND DISCUSSION

3.1. Thermal Properties. *3.1.1. TGA Measurements.* Figure 1 shows the thermal degradation behaviors of PLLA and PLLA/PDLLA blends by TGA measurement under a nitrogen atmosphere at 10 °C/min. The thermal onset of degradation temperatures of neat PLLA, 90/10, 70/30, 50/50, 30/70 wt % PLLA/PDLLA blends, and PDLLA is 287, 280, 278, 278, 276, 269 °C, respectively. It was found that lower degradation temperatures occurred with higher percentages of PDLLA, which is probably due to the lower activation energy of thermal degradation with lower molecular weight of PDLLA.[38]

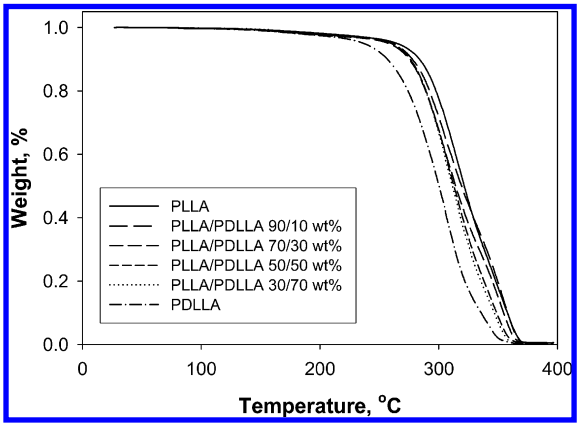

Figure 1. TGA curves of PLLA and its blends.

3.1.2. DSC Measurements. The DSC heating curves of PLLA and its blends at a rate of 5 °C/min are presented in Figure 2. The glass transition temperatures (T_g) of neat PLLA and PDLLA are 50 and 43 °C, respectively. There is no crystallization and melting peak observed for neat PDLLA in DSC measurements, which verifies its amorphous nature. A glass transition at 40−50 °C, a crystallization peak at 80−120 °C, and a melting peak at around 168 °C are detected for neat PLLA and PLLA/PDLLA blends. All the blends with different ratios exhibit a single T_g that shifts to a lower temperature with increasing the PDLLA content. In the blends, no broadening in the peak of T_g is observed. These results suggest that PLLA and PDLLA are miscible in the molten state.[39]

Addition of PDLLA to PLLA significantly affects the crystallization behavior in PLLA. As shown in Figure 2, the crystallization temperature (T_c) shifts from 88 to 103 °C with an increase in PDLLA content, which suggests an extra energy is needed for PLLA crystallization from glassy state due to the dilution effects of PDLLA on the PLLA component. Therefore, a higher temperature is needed for the PLLA component to grow crystal.[40]

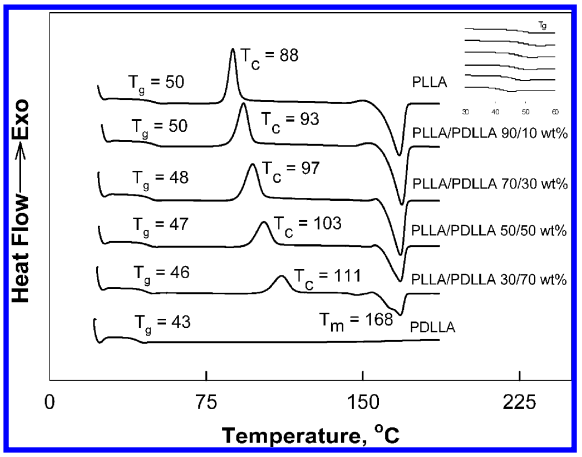

Figure 2. DSC thermogram of PLLA and its blends.

3.2. CO_2 Induced Crystallization. As CO_2 can plasticize glassy polymers, it can also affect semicrystalline polymers by plasticizing the amorphous phase. The plasticization of the amorphous phase increases the mobility of polymer chains, which allows the chains to rearrange into a more ordered state, resulting in crystallization.[41−44] PLLA is a semicrystalline polymer, and it has been reported that conditioning PLLA with CO_2 can result in crystallization at a lower saturation temperature.[10,11,45,46] As revealed by X-ray diffraction patterns (data not presented), PLLA and PLLA/PDLLA blends prepared by ice water quench were amorphous, but crystalline domains formed in the samples after contact with CO_2 at certain pressure. The crystallinities of PLLA and its blends saturated with CO_2 at 0 °C for 24 h at different pressures were derived from the X-ray diffraction patterns and are presented in Figure 3. The crystallinity of samples decreases with the addition of PDLLA component. It is shown that the crystalline content increases with increasing CO_2 pressure. At the pressure lower than 1.4 MPa, no crystallization of PLLA blends induced by CO_2 was observed. Controlling the gas pressure allows the changes in the degree of plasticization and swelling of polymers; consequently, the free volume and the mobility of

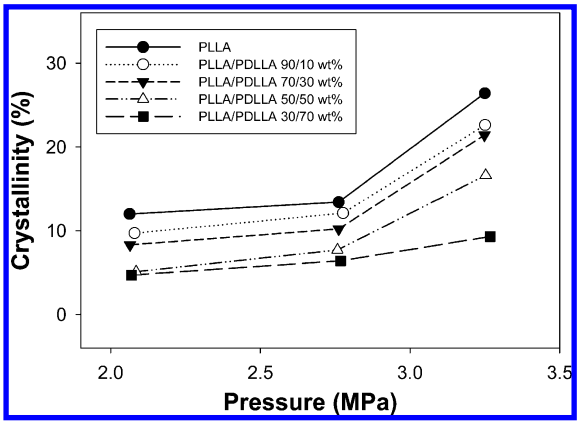

Figure 3. Crystallinity of PLLA and its blends saturated with CO_2 at 0 °C for 24 h at different pressures.

dx.doi.org/10.1021/ie3000997 | Ind. Eng. Chem. Res. 2012, 51, 6722−6730

polymer chains will be affected. The free volume of polymer and mobility of polymer chains increase with increasing pressure, which induces the chains to reorganize to a lower free energy crystalline structure and thus high crystallinity is obtained.

3.3. CO_2 Solubility and Diffusion Coefficient in PLLA and Its Blends. Substantial solubility of CO_2 controls bubble nucleation and formation of a porous structure.[37] In order to examine the dominate effect on foam morphologies, the CO_2 solubility and diffusion coefficient in PLLA and its blend samples were investigated. The sorption kinetics of CO_2 in PLLA and PLLA/PDLLA blends in the ratios 90/10, 70/30, 50/50, and 30/70 wt % were investigated by recording the changes of gas mass uptake in the polymer over time until a stable value was obtained. Since CO_2 induced crystallization in PLLA and PLLA/PDLLA blends and the crystalline phase in polymer does not absorb gas, the equilibrium solubility and diffusion coefficient data in PLLA and its blends are corrected for the unit mass of the amorphous region.[10,11]

The solubility of CO_2 in PLLA and blends at 0 °C at an equilibrium pressure up to 2.8 MPa is shown in Figure 4. The

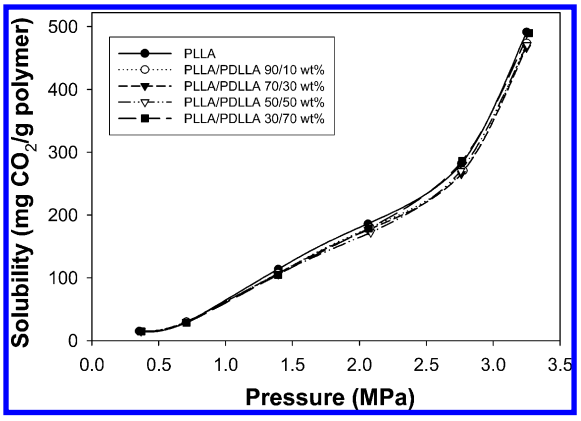

Figure 4. Solubility of CO_2 in PLLA and its blends at 0 °C.

solubility increases with increasing pressure. The increase in gas solubility is attributed to the high degree of plasticization in the amorphous phase with increasing pressure. CO_2 gas sorption in polymer is a purely physical phenomenon that is related to the polymer structure. The solubility of CO_2 in PLLA is much higher than other polymers such as polystyrene (PS) and polyethylene (PE) under the same experimental condition due to the specific intermolecular interactions between CO_2 and the electro-donating functional (e.g., carbonyl) groups that form an electron donor−acceptor complex.[10,47,48] Since PLLA and PDLLA are isomers with same chemical structures and same kinds of bonds between atoms, the similar sorption behavior of CO_2 gas in the amorphous phase of PLLA and PLLA/PDLLA blends is reasonable.

Diffusion coefficients at various pressures were obtained by fitting the sorption kinetic data to a hybrid model that combines both short and long-term Fickian diffusion[35] (Figure 5). The diffusion coefficient increases with increasing pressure. A sharp change in diffusion coefficient from 1.4 to 2.1 MPa is probably due to PLLA and PLLA/PDLLA blends undergoing a transition from glassy to rubbery state. Such transition has been observed in PMMA−CO_2 system because of the specific interaction of carbonyl groups with CO_2.[37] The diffusivity behaviors of CO_2 in PLLA and its blends are similar but exhibit

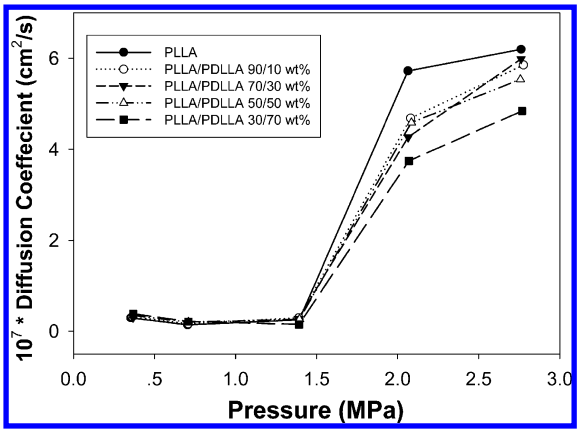

Figure 5. Diffusion coefficient of CO_2 in PLLA and its blends at 0 °C.

a weak dependence on the PLLA and PDLLA ratio. The increase in diffusion coefficient may be attributed to the small changes in the free void between phase boundaries as a result of increase in crystallinity of samples treated in CO_2 with increasing of PLLA content.

3.4. Porosity. Porosity is defined as the percentage of void space in a solid. High porosity is required for scaffolds to provide adequate space for cell seeding and growth. To investigate the foaming behaviors, PLLA and its blends were saturated with CO_2 at 2.8 MPa and 0 °C for 24 h and subsequently foamed in the temperature range 30−90 °C. The porosities obtained as a function of foaming temperatures are presented in Figure 6. Foaming started at lower temperatures

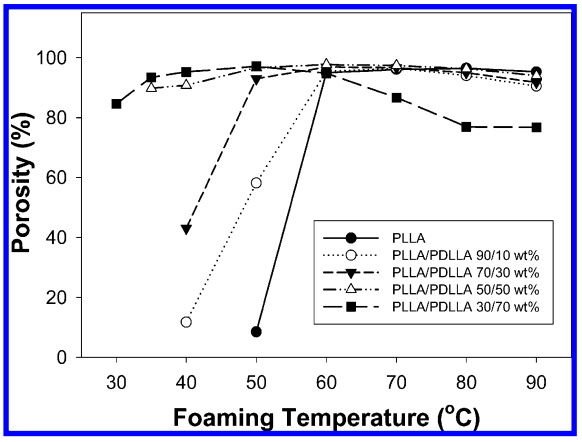

Figure 6. Porosities of PLLA and its blends foams (samples saturated at 2.8 MPa and 0 °C for 24 h) as a function of foaming temperature.

with increasing PDLLA content. The temperature at which the porosity of sample began to increase was defined as the foaming starting temperature. The foaming starting temperature of PLLA, 90/10, 70/30, 50/50, and 30/70 wt % PLLA/PDLLA blends is 50, 40, 40, 35, and 30 °C with porosities 8%, 12%, 43%, 90%, and 85%, respectively. The foaming starting temperature corresponds to the T_g of the polymer/gas mixture and depends strongly on the CO_2 content in the sample in amorphous polymer.[49] Also, the crystallization and the resulting change in viscoelastic behavior played a major role in foaming process. As the T_g of PLLA and its blends, solubility of CO_2, and the gas diffusion in the polymer matrix are similar, the pore nucleation and growth is attributed to the viscoelastic behavior of the matrix.[50,51] The stiffness of the polymer matrix is

dx.doi.org/10.1021/ie3000997 | Ind. Eng. Chem. Res. 2012, 51, 6722−6730

controlled by the crystallinity and increase with increasing crystallinity.[52] Therefore, higher temperature is needed to overcome the activation energy barrier to form detectable gas bubbles in the matrix with higher crystallinity content. Since the addition of PDLLA resulted in a lower crystallinity in the blend (Figure 3), pore nucleation and growth occurred at lower temperatures with increasing PDLLA content. The porosity increases with increasing foaming temperature and a maximum porosity ~96% is obtained for PLLA and its blends.

With increasing foaming temperature from 30 to 50 °C, the porosity of 30/70 wt % blend increases from 85% to 97%. Further increasing the foaming temperature beyond 50 °C resulted in the porosity of 30/70 wt % PLLA/PDLLA sample to drop due to the pore collapse at higher temperature. The deformation of the samples was confirmed with SEM. The 30/70 wt % sample shows well-developed foam structure at 30 and 40 °C with closed pores. With an increase in temperature up to 50 °C, the pores collapsed (photo not present). However, only a slightly decrease in the porosity of PLLA, 90/10, 70/30, and 50/50 wt % blends with an increase in foaming temperature is observed, which probably is attributed to the higher crystallinity thus higher chain modulus in the samples.

3.5. Formation of Open Pore Foam Morphologies. Matrix with porous surfaces and interconnected pore structures is often required in bioengineering applications,[8] which allows cells in the host tissue to interact freely with transplanted cells and reduces diffusion barriers of metabolites between engineered and surrounding tissues. The disadvantage of scaffold prepared in CO_2 is that it yields mostly a closed-pore structure. Since the interaction of PS with CO_2 and the resultant foaming morphology have been widely studied,[4,5] the foam morphology of PS was used as a comparison in this work. The PS sample saturated at 2.8 MPa and 0 °C for 24 h and subsequently foamed at 80 °C shows a closed-pore in the core and a nonporous skin layer around the sample surface (Figure 7a_1 and a_2), which is the typical foam morphology obtained through CO_2 gas foaming. When the pressure is released and/or during the time before the heating step is employed, CO_2 will desorb from the polymer sample. The rapid diffusion of CO_2 out of the sample creates a depletion layer near the edges in which the gas concentration is too low to contribute significantly to bubble nucleation and growth. Therefore, the foamed sample normally exhibits dense (unfoamed) surface layers and porous cores.[53] However, an important requirement for a porous tissue scaffold is a high degree of interconnectivity between the pores, which enable cells to migrate through the scaffold.[54] Both closed pores and a nonporous surface may provide barriers for diffusion, which will prevent cells from migrating between the inferior and exterior of the matrices.

In PLLA and its blend samples, the dense skin layer was not observed at all the experimental conditions. The skinless porous morphologies of 70/30 wt % PLLA/PDLLA samples foamed in the range of 50−90 °C are presented in Figure 7b−e. The solubility of CO_2 in 70/30 wt % blend at 2.8 MPa and 0 °C is 265 mg CO_2/g polymer, which is about two times of the solubility of CO_2 (140 mg CO_2/g polymer) in PS at the same saturation conditions. The skinless morphologies created in PLLA/PDLLA blends therefore can be attributed to the high solubility of CO_2, which provide enough gas for pore nucleation and growth in the skin. The 70/30 wt % PLLA/PDLLA blend sample saturated with CO_2 at 2.8 MPa and 0 °C and subsequently foamed at 50 °C exhibits an interconnected pore structure in the core section (Figure 7b_1). The dense skin

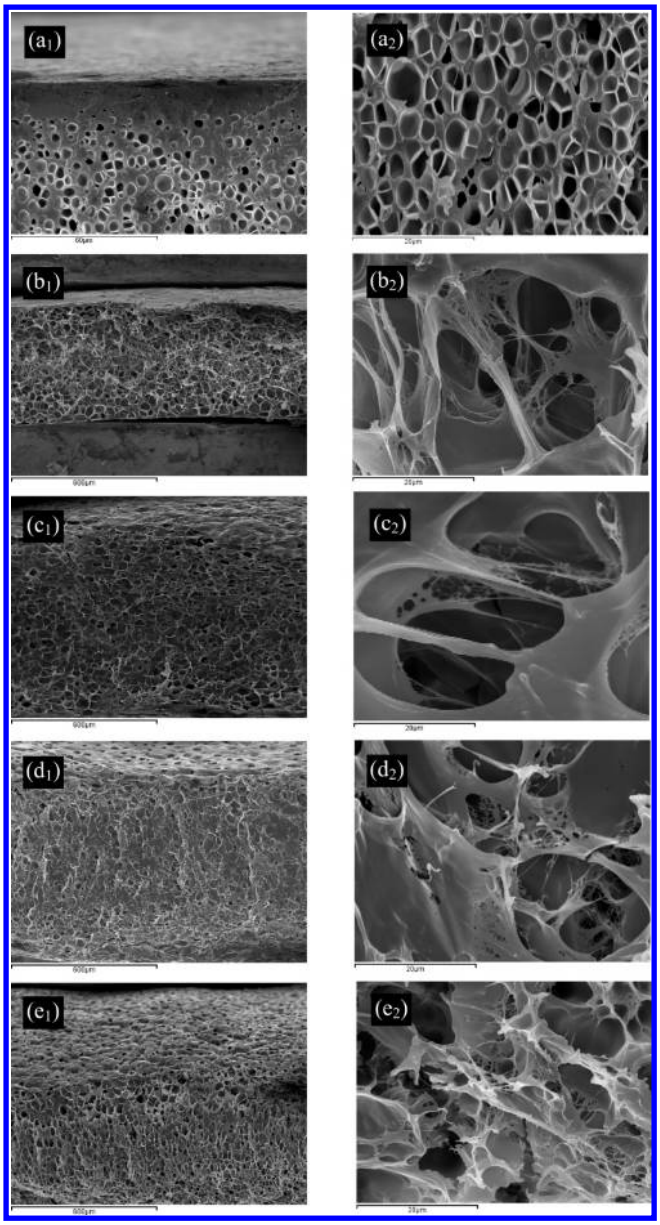

Figure 7. SEM microphotographs (a_1) surface cross section ×1000 and (a_2) cross section ×2500 of PS saturated at 2.8 MPa and 0 °C for 24 h, foamed at 80 °C; and PLLA/PDLLA 70/30 wt % blend saturated at 2.8 MPa and 0 °C for 24 h, foamed at (b_1) 50 °C, surface cross section ×100; (b_2) 50 °C, cross section ×2500; (c_1) 70 °C, surface cross section ×100; (c_2) 70 °C, cross section ×2500; (d_1) 80 °C, surface cross section ×100; (d_2) 80 °C, cross section ×2500; (e_1) 90 °C, surface cross section ×100; (e_2) 90 °C, cross section ×2500.

layer disappears, but the surface is remaining nonporous (Figure 7b_2). The influence of temperature on the foam morphology is an important processing parameter because it affects the nucleation rate as well as the viscosity of matrices. The increased temperature induces a greater thermodynamic instability and reduced the viscosity thus a highly interconnected and open morphology with somewhat porous surface is obtained when sample foamed at 70 °C (Figure 7c_1 and c_2). The 70/30 wt % sample conditioned with CO_2 and foamed at 80 °C displays an interconnected pore structure (10−50 μm) in the cross section and an intriguing porous surface on the exterior layer (Figure 7d_1 and d_2). With a further increase in foaming temperature to 90 °C, more pores are observed on the

dx.doi.org/10.1021/ie3000997 | Ind. Eng. Chem. Res. 2012, 51, 6722−6730

surface (Figure 7e$_1$ and e$_2$). The details of the surface morphology of 70/30 wt % blend samples are presented in Figure 8. The sample foamed at 80 °C shows smooth pores

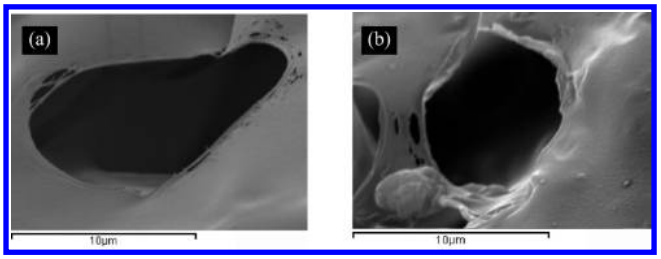

Figure 8. SEM microphotographs of the surface of PLLA/PDLLA 70/30 wt % blend saturated at 2.8 MPa and 0 °C for 24 h, foamed at (a) 80 °C, × 5000; (b) 90 °C, × 5000.

with size of ~10 μm on the surface (Figure 8a). With increasing foaming temperature to 90 °C, smaller pores (~6 μm) with rough edge on the surface are observed (Figure 8b).

The temperature window to obtain porous structure for various PLLA/PDLLA blends is summarized in Figure 9. The

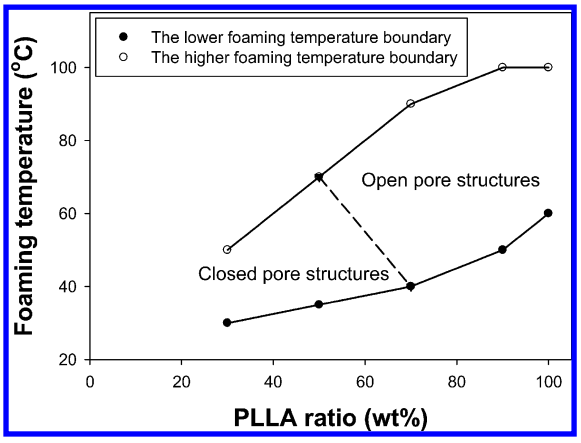

Figure 9. Foaming temperature window as a function of the PLLA/PDLLA ratio. Samples saturated with CO_2 at 2.8 MPa and 0 °C for 24 h.

30/70 wt % PLLA/PDLLA sample started to foam at 30 °C, but the pores collapsed when the foaming temperature was higher than 50 °C. With increasing the PLLA content, the temperature to produce well-developed porous structure increased due to the higher crystallinity thus higher material stiffness. It can be seen from Figure 9 that the 30/70 wt % PLLA/PDLLA sample only generated closed pores. With an increase in PLLA ratio, the 50/50 wt % sample created porous structure with interconnected pores at 70 °C. Further increasing the PLLA content, although the temperature to obtain well porous structure increased, all samples produced open pore structures in the foaming window (Figure 9). Pore morphologies strongly depend on the dissolved amount of gas available in the sample. It has been reported that poly(ether imide), poly(ether sulfone), and polyimide/polysulfone blend[49] exhibited a transition from a closed pore structure to an open pore morphology if the CO_2 concentration raised above a critical value. With increasing the solubility of CO_2 in the polymer, the concentration of nucleation points is increased. Therefore, it is possible to produce a more interconnected pore structure and a porous skin by dissolving a greater amount of gas in polymer matrices. It has been demonstrated the solubility of CO_2 in PLLA is much higher than that in PMMA and PS, and partially open porous structures have been obtained in our previous investigation.[10,11] As the solubility of PLLA and its blends are similar (Figure 4), the high CO_2 solubility is not the only reason for the formation of open pore structure. Crystallization has been demonstrated as one of the major parameters to control the foaming morphologies of semicrystalline polymers. The crystalline phase would act as a nucleation agent in specific conditions and enhance the matrix stiffness. Park et al.[55] reported an open pore low-density polyethylene (LDPE) and LDPE/PS foams that was induced by a hard/soft system. The hard sections assisted in maintaining the shape of pores and the overall foam structure, while the soft sections could open up the wall of pores during pore growth. In semicrystalline polymer/gas system, the crystalline phase might also serve as the hard sections to keep the shape of pores and the amorphous soft phase could break up the wall of pores.

The foam morphologies of polymers with different blend compositions treated with CO_2 at 2.8 MPa and 0 °C for 24 h and subsequently foamed at 80 °C are shown in Figures 10 and

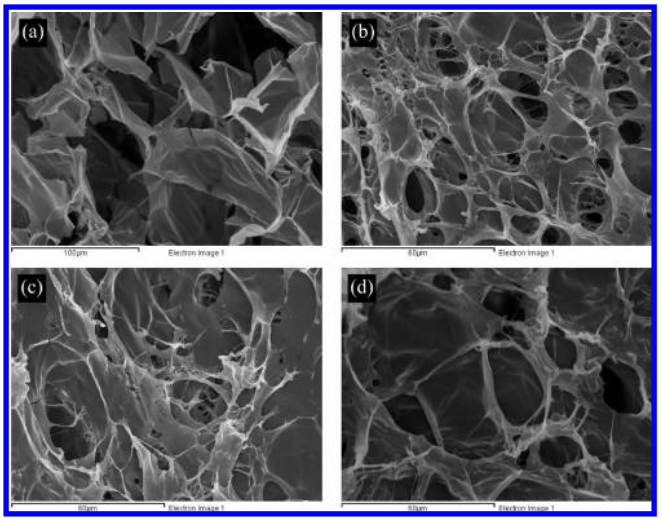

Figure 10. SEM microphotographs of the cross section of samples saturated with CO_2 at 2.8 MPa and 0 °C for 24 h, foamed at 80 °C (a) PLLA; (b) PLLA/PDLLA 90/10 wt %; (c) PLLA/PDLLA 70/30 wt %; (d) PLLA/PDLLA 50/50 wt %.

11. Neat PLLA exhibited partially interconnected pore morphologies with the pore size about 20−50 μm in the core (Figure 10a) and nonuniform limited pores on the surface (Figure 11a). A large amount of open and interconnected pores is obtained with the addition of 10 wt % PDLLA (Figures 10b and 11b). No improvement of the pore formation on the surface is observed. With an increase in PDLLA to 30 wt %, the foam obtained shows an increase in interconnectivity of pores while the pore size is similar compared to the neat PLLA foams (Figure 10c). Moreover, a smooth and uniform porous surface is obtained (Figure 11c). Further increase PDLLA content to 50 wt %, the sample shows partially open pore structure with the pore size about 20−100 μm (Figure 10d). The surface of 50 wt % PLLA/PDLLA sample exhibits some unbroken protruding foam bubbles (Figure 11d), which is probably due to the higher flexibility of chains with higher PDLLA content.

In the presence of CO_2, the physical property changes occur in PLLA, which affects its foam morphology. The solubility of

dx.doi.org/10.1021/ie3000997 | Ind. Eng. Chem. Res. 2012, 51, 6722−6730

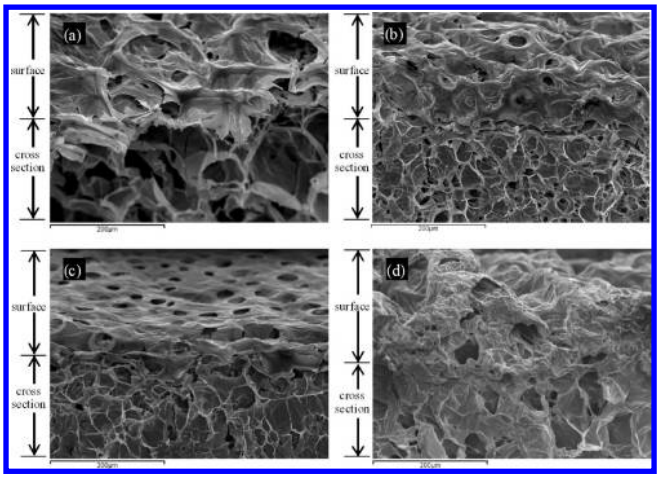

Figure 11. SEM microphotographs of the surface cross section of samples saturated with CO_2 at 2.8 MPa and 0 °C for 24 h, foamed at 80 °C (a) PLLA; (b) PLLA/PDLLA 90/10 wt %; (c) PLLA/PDLLA 70/30 wt %; (d) PLLA/PDLLA 50/50 wt %.

CO_2 in sample also affects bubble nucleation and formation of a porous structure. X-ray diffraction data obtained for PLLA and blend samples treated with CO_2 revealed formation of crystalline domains in the samples after contact with CO_2 (Figure 3). CO_2 induced crystallization plays a major role on the foam processing through its effects on the pore nucleation mechanism resulting in larger pore densities due to heterogeneous nucleation at the amorphous/crystalline boundaries and the pore growth mechanism resulting in smaller pore sizes due to the increased matrix stiffness.[56] The solubility of CO_2 in PLLA and blends was found to be similar (Figure 4). Crystallization of PLLA induced by CO_2 thus effects on the foam morphology have been observed. Material stiffness in polymers is directly proportional to crystallinity of the matrix. Addition of PDLLA into PLLA decreases the crystallization of PLLA as the results presented in Figure 3. As adding PDLLA into PLLA influences the material stiffness, variations in morphologies obtained of various blends are related to physical properties induced by CO_2. Therefore, by controlling the blend ratio and foaming conditions thus the physical properties of the blend samples, the open and interconnected pore structure could be obtained by only using CO_2 as a physical blowing agent. The surface morphologies of samples with different PLLA and PDLLA ratio indicated the brittleness of PLLA blends decreased with increasing of PDLLA content. Materials with specific material stiffness and flexibility as well as high gas solubility are required to obtain completely interconnected pore morphologies using CO_2 as foaming agent.

4. CONCLUSION

Based upon X-ray diffraction analysis, it was found that CO_2 induced crystallization in PLLA and its blends. The crystallinity increases with increasing pressure and decreases with an increase in the ratio of PDLLA. The solubility and the diffusional behaviors of PLLA and its blends are similar. The foaming starting temperature of samples decreased with an increase in PDLLA content. The porosity of PLLA/PDLLA 30/70 wt % sample drops when foaming temperature is higher than 50 °C due to the collapse of pores. With a decrease in the PDLLA content, only a slight decrease in the porosity of PLLA and its blends was observed. Using CO_2 as a physical blowing agent to prepare polymer foams normally lead to a closed pore structure in the core and an apparently nonporous skin. Simple changes in PLLA and PDLLA ratio and CO_2 processing conditions, scaffolds with well-interconnected porous surface and core structure were fabricated in PLLA/PDLLA blend by means of a one step process. Results indicated that materials with optimum material stiffness and flexibility as well as high gas solubility are required to obtain well interconnected pore morphologies using CO_2 as foaming agent.

AUTHOR INFORMATION

Corresponding Author

*Tel.: 86-28-8540 8361. E-mail: xliao@scu.edu.cn.

Present Address

[§]Sealed Air Corporation, 2401 Dillard Street, Grand Prairie, TX 75051, United States

Notes

The authors declare no competing financial interest.

REFERENCES

(1) Mikos, A. G.; Thorsen, A. J.; Czerwonka, L. A.; Bao, Y.; Langer, R.; Winslow, D. N.; Vacanti, J. P. Preparation and characterization of poly(L-lactic acid) foams. *Polymer* **1994**, *35*, 1068−1077.

(2) Martina, M.; Hutmacher, D. W. Biodegradable polymers applied in tissue engineering research: a review. *Polym. Int.* **2007**, *56* (2), 145−157.

(3) Rezwan, K.; Chen, Q. Z.; Blaker, J. J.; Boccaccini, A. R. Biodegradable and bioactive porous polymer/inorganic composite scaffolds for bone tissue engineering. *Biomaterials* **2006**, *27* (18), 3413−3431.

(4) Arora, K. A.; Lesser, A. J.; McCarthy, T. J. Preparation and characterization of microcellular polystyrene foams processed in supercritical carbon dioxide. *Macromolecules* **1998**, *31* (14), 4614−4620.

(5) Leung, S. N.; Wong, A.; Guo, Q. P.; Park, C. B.; Zong, J. H. Change in the critical nucleation radius and its impact on cell stability during polymeric foaming processes. *Chem. Eng. Sci.* **2009**, *64* (23), 4899−4907.

(6) Kirby, C. F.; McHugh, M. A. Phase behavior of polymers in supercritical fluid solvents. *Chem. Rev.* **1999**, *99* (2), 565−602.

(7) Canelas, D. A.; Burke, A. L. C.; DeSimone, J. M. Carbon dioxide as a continuous phase for polymer synthesis. *Plast. Eng.* **1997**, *53* (12), 37−40.

(8) Mooney, D. J.; Baldwin, D. F.; Suh, N. P.; Vacanti, L. P.; Langer, R. Novel approach to fabricate porous sponges of poly(D,L-lactic-co-glycolic acid) without the use of organic solvents. *Biomaterials* **1996**, *17* (14), 1417−1422.

(9) Lips, P. A. M.; Velthoen, I. W.; Dijkstra, P. J.; Wessling, M.; Feijen, J. Gas foaming of segmented poly(ester amide) films. *Polymer* **2005**, *46* (22), 9396−9403.

(10) Liao, X.; Nawaby, A. V.; Whitfield, P.; Day, M.; Champagne, M.; Denault, J. Layered open pore poly(L-lactic acid) nanomorphology. *Biomacromolecules* **2006**, *7* (11), 2937−2941.

(11) Liao, X.; Nawaby, A. V.; Whitfield, P. S. Carbon dioxide-induced crystallization in poly(L-lactic acid) and its effect on foam morphologies. *Polym. Int.* **2010**, *59*, 1709−1718.

(12) Corre, Y. M.; Maazouz, A.; Duchet, J.; Reignier, J. Batch foaming of chain extended PLA with supercritical CO_2: Influence of the rheological properties and the process parameters on the cellular structure. *J. Supercrit. Fluids* **2011**, *58* (1), 177−188.

(13) Jenkins, M. J.; Harrison, K. L.; Silva, M. M. C. G.; Whitaker, M. J.; Shakesheff, K. M.; Howdle, S. M. Characterisation of microcellular foams produced from semi-crystalline PCL using supercritical carbon dioxide. *Eur. Polym. J.* **2006**, *42* (11), 3145−3151.

(14) Nawaby, A. V.; Farah, A. A.; Liao, X.; Pietro, W. J.; Day, M. Biodegradable open cell foams of telechelic poly(epsilon-caprolactone)

macroligand with ruthenium(II) chromophoric subunits via subcritical CO_2 processing. *Biomacromolecules* **2005**, *6* (5), 2458−2461.
(15) Salerno, A.; Di Maio, E.; Iannace, S.; Netti, P. A. Solid-state supercritical CO_2 foaming of PCL and PCL-HA nano-composite: Effect of composition, thermal history and foaming process on foam pore structure. *J. Supercrit. Fluids* **2011**, *58* (1), 158−167.
(16) Gualandi, C.; White, L. J.; Chen, L.; Gross, R. A.; Shakesheff, K. M.; Howdle, S. M.; Scandola, M. Scaffold for tissue engineering fabricated by non-isothermal supercritical carbon dioxide foaming of a highly crystalline polyester. *Acta Biomater.* **2010**, *6* (1), 130−136.
(17) Salerno, A.; Iannace, S.; Netti, P. A. Open-pore biodegradable foams prepared via gas foaming and microparticulate templating. *Macromol. Biosci.* **2008**, *8* (7), 655−664.
(18) Harris, L. D.; Kim, B. S.; Mooney, D. J. Open pore biodegradable matrices formed with gas foaming. *J. Biomed. Mater. Res.* **1998**, *42* (3), 396−402.
(19) Nam, Y. S.; Yoon, J. J.; Park, T. G. A novel fabrication method of macroporous biodegradable polymer scaffolds using gas foaming salt as a porogen additive. *J. Biomed. Mater. Res.* **2000**, *53* (1), 1−7.
(20) Murphy, W. L.; Dennis, R. G.; Kileny, J. L.; Mooney, D. J. Salt fusion: An approach to improve pore interconnectivity within tissue engineering scaffolds. *Tissue Eng.* **2002**, *8* (1), 43−52.
(21) Collins, N. J.; Bridson, R. H.; Leeke, G. A.; Grover, L. M. Particle seeding enhances interconnectivity in polymeric scaffolds foamed using supercritical CO_2. *Acta Biomater.* **2010**, *6* (3), 1055−1060.
(22) Wang, X. X.; Li, W.; Kumar, V. A method for solvent-free fabrication of porous polymer using solid-state foaming and ultrasound for tissue engineering applications. *Biomaterials* **2006**, *27* (9), 1924−1929.
(23) Morisaki, M.; Ito, T.; Hayvali, A.; Tabata, I.; Hisada, K.; Hori, T. Preparation of skinless polymer foam with supercritical carbon dioxide and its application to a photoinduced hydrogen evolution system. *Polymer* **2008**, *49* (6), 1611−1619.
(24) Kricheldorf, H. R.; Berl, M.; Scharngal, N. Poly(lactones). 9. Polymerization mechanism of metal alkoxide initiated polymerizations of lactide and various lactones. *Macromolecules* **1988**, *21*, 286−293.
(25) Lehermeier, H. J.; Dorgan, J. R.; Way, J. D. Gas permeation properties of poly(lactic acid). *J. Membr. Sci.* **2001**, *190* (2), 243−251.
(26) Urayama, H.; Kanamori, T.; Kimura, Y. Properties and biodegradability of polymer blends of poly(L-lactide)s with different optical purity of the lactate units. *Macromol. Mater. Eng.* **2002**, *287* (2), 116−121.
(27) Avella, M.; Errico, M. E.; Immirzi, B.; Malinconico, M.; Martuscelli, E.; Paolillo, L.; Falcigno, L. Radical polymerization of poly(butyl acrylate) in the presence of poly(L-lactic acid) 0.1. Synthesis, characterization and properties of blends. *Angew. Makromol. Chem.* **1997**, *246*, 49−63.
(28) Baratian, S.; Hall, E. S.; Lin, J. S.; Xu, R.; Runt, J. Crystalization and solid-state structure of random polylactide copolymers: Poly(L-lactide-co-D-lactide)s. *Macromolecules* **2001**, *34* (14), 4857−4864.
(29) Schiller, C.; Rasche, C.; Wehmoller, M.; Beckmann, F.; Eufinger, H.; Epple, M.; Weihe, S. Geometrically structured implants for cranial reconstruction made of biodegradable polyesters and calcium phosphate/calcium carbonate. *Biomaterials* **2004**, *25* (7−8), 1239−1247.
(30) Li, D. C.; Liu, T.; Zhao, L.; Lian, X. S.; Yuan, W. K. Foaming of poly(lactic acid) based on its nonisothermal crystallization behavior under compressed carbon dioxide. *Ind. Eng. Chem. Res.* **2011**, *50* (4), 1997−2007.
(31) Mihai, M.; Huneault, M. A.; Favis, B. D. Rheology and extrusion foaming of chain-branched poly(lactic acid). *Polym. Eng. Sci.* **2010**, *50* (3), 629−642.
(32) Reignier, J.; Gendron, R.; Champagne, M. F. Extrusion foaming of poly(lactic acid) blown with Co-2: Toward 100% green material. *Cell. Polym.* **2007**, *26* (2), 83−115.
(33) Liao, X.; Nawaby, A. V.; Handa, Y. P. Layered and cellular morphologies in atactic/syndiotactic polystyrene blends. *Cell. Polym.* **2007**, *26* (2), 69−81.
(34) Mizumoto, T.; Sugimura, N.; Moritani, M.; Sato, Y.; Masuoka, H. CO_2-induced stereocomplex formation of stereoregular poly(methyl methacrylate) and microcellular foams. *Macromolecules* **2000**, *33* (18), 6757−6763.
(35) Wong, B.; Zhang, Z. Y.; Handa, Y. P. High-precision gravimetric technique for determining the solubility and diffusivity of gases in polymers. *J. Polym. Sci., Polym. Phys.* **1998**, *36* (12), 2025−2032.
(36) Angus, S.; Armstrong, B.; de Reuck, K. M. International Union of Pure and Applied Chemistry. Carbon Dioxide International Thermodynamic Tables of the Fluid State; Permagon of Canada Ltd.: Toronto, Canada, 1976; Vol. 3.
(37) Handa, Y. P.; Zhang, Z.; Wong, B. Solubility, diffusivity, and retrograde vitrification in PMMA-CO_2, and development of submicron cellular structures. *Cell. Polym.* **2001**, *20* (1), 1−16.
(38) Yang, M. H.; Lin, Y. H. Measurement and silulation of thermal stability of poly(lactic acid) by thermogravimetric analysis. *J. Test. Eval.* **2009**, *37* (4), 1−6.
(39) Ren, J. D.; Adachi, K. Dielectric relaxation in blends of amorphous poly(DL-lactic acid) and semicrystalline poly(L-lactic acid). *Macromolecules* **2003**, *36* (14), 5180−5186.
(40) Pan, P.; Liang, Z.; Zhu, B.; Dong, T.; Inoue, Y. Blending effects on polymorphic crystallization of poly(L-lactide). *Macromolecules* **2009**, *42* (9), 3374−3380.
(41) Handa, Y. P.; Zhang, Z. Y.; Roovers, L. Compressed-gas-induced crystallization in tert-butyl poly(ether ether ketone). *J. Polym. Sci., Polym. Phys.* **2001**, *39* (13), 1505−1512.
(42) Handa, Y. P.; Zhang, Z. Y.; Wong, B. Effect of compressed CO_2 on phase transitions and polymorphism in syndiotactic polystyrene. *Macromolecules* **1997**, *30* (26), 8499−8504.
(43) Schultze, J. D.; Engelmann, I. A. D.; Boehning, M.; Springer, J. Influence of sorbed carbon dioxide on transition temperatures of poly(p-phenylene sulphide). *Polym. Adv. Technol.* **1991**, *2* (3), 123−126.
(44) Beckman, E.; Porter, R. S. Crystallization of bisphenol a polycarbonate induced by supercritical carbon dioxide. *J. Polym. Sci., Polym. Phys.* **1987**, *25* (7), 1511−1517.
(45) Sato, Y.; Yamane, M.; Sorakubo, A.; Takishima, S.; Masuoka, H.; Yamamoto, H.; Takasugi, M. Solubility and Diffusion Coefficient of Carbon Dioxide in Polylactide. In *The 21st Japan Symposium on Thermophysical Properties*; Nagoya, Japan, 2000; pp 196−198.
(46) Takada, M.; Hasegawa, S.; Ohshima, M. Crystallization kinetics of poly(L-lactide) in contact with pressurized CO_2. *Polym. Eng. Sci.* **2004**, *44* (1), 186−196.
(47) Kazarian, S. G.; Vincent, M. F.; Bright, F. V.; Liotta, C. L.; Eckert, C. A. Specific intermolecular interaction of carbon dioxide with polymers. *J. Am. Chem. Soc.* **1996**, *118* (7), 1729−1736.
(48) Kazarian, S. G. Polymers and supercritical fluids: Opportunities for vibrational spectroscopy. *Macromol. Symp.* **2002**, *184*, 215−228.
(49) Krause, B.; Diekmann, K.; van der Vegt, N. F. A.; Wessling, M. Open nanoporous morphologies from polymeric blends by carbon dioxide foaming. *Macromolecules* **2002**, *35* (5), 1738−1745.
(50) Baldwin, D. F.; Park, C. B.; Suh, N. P. A microcellular processing study of poly(ethylene terephthalate) in the amorphous and semicrystalline states 0.1. Microcell nucleation. *Polym. Eng. Sci.* **1996**, *36* (11), 1437−1445.
(51) Baldwin, D. F.; Park, C. B.; Suh, N. P. A microcellular processing study of poly(ethylene terephthalate) in the amorphous and semicrystalline states 0.2. Cell growth and process design. *Polym. Eng. Sci.* **1996**, *36* (11), 1446−1453.
(52) Doroudiani, S.; Park, C. B.; Kortschot, M. T. Effect of the crystallinity and morphology on the microcellular foam structure of semicrystalline polymers. *Polym. Eng. Sci.* **1996**, *36* (21), 2645−2662.
(53) Kumar, V.; Weller, J. E. Creating an unfoamed skin on microcellular foams. *SPE ANTEC Tech.* **1992**, *38*, 1508−1512.
(54) Wake, M. C.; Gupta, P. K.; Mikos, A. G. Fabrication of pliable biodegradable polymer foams to engineer soft tissues. *Cell. Transplant* **1996**, *5* (4), 465−473.

(55) Park, C. B.; Padareva, V.; Lee, P. C.; Naguib, H. E. Extruded open-celled LDPE-based foams using non-homogeneous melt structure. *J. Polym. Eng.* **2005**, *25* (3), 239−260.
(56) Baldwin, D. F.; Shimbo, M.; Suh, N. P. The role of gas dissolution and induced crystallization during microcellular polymer processing - a study of poly(ethylene-terephthalate) and carbon-dioxide systems. *J. Eng. Mater. Technol.* **1995**, *117* (1), 62−74.